Synchronization of OFDM at low SNR over an AWGN channel

André B.J. Kokkeler, Gerard J.M. Smit

University of Twente
Department of Electrical Engineering,
Computer Science and Mathematics,
P.O. Box 217,
7500 AE Enschede,
The Netherlands

Abstract. This paper is based on Extended Symbol OFDM (ES-OFDM) where symbols are extended in time. This way ES-OFDM can operate at low SNR. Each doubling of the symbol length improves the SNR performance by 3 dB in case of a coherent receiver. One of the basic questions is how to synchronize to signals far below the noise floor. An algorithm is presented which is based on the transmission of pilot symbols. At the receiver, the received signal is cross correlated with the known pilot symbol and the maximum magnitude is determined. The position of the maximum value within the cross correlation function indicates the time difference between transmitter and receiver. The performance of the algorithm in case of an Additive White Gaussian Noise (AWGN) channel, is assessed based on a theoretical approximation of the probability of correct detection of the time difference. The theoretical approximation matches with simulation results and shows that synchronization can be achieved for low (negative) SNRs.

Keywords: Correlation, Differential phase shift keying, Fourier transforms, Frequency division multiplexing, Modulation

1 Introduction

Orthogonal Frequency Division Multiplexing (OFDM) is the most popular multi carrier transmission scheme for already quite some years. It is being used in e.g. IEEE802.11a and 3GPPLTE [1]. In OFDM systems, data is spread over a large number of orthogonal carriers, each being modulated at a low bit rate. The modulation scheme for the carriers can be selected among e.g. multilevel-QAM, QPSK or BPSK, dependent on the channel conditions and the noise level at the receiver. Given a modulation scheme, a transmitter has to use a minimum amount of transmit energy to achieve acceptable Bit Error Rates (BERs) [2]. In case the power budget at the transmitter is constant, increasing noise levels at the receiver are generally counteracted by lowering the modulation level. Once arrived at the lowest modulation level (BPSK), other techniques have to be used to combat worsening noise conditions. In [3] and [4], repetition of symbols in

time is analyzed. By means of Maximum Ratio Combining, multiple replicas of symbols are used to lower the BER, also lowering the bit rate. In [5], repetition of data in the frequency domain is elaborated.

However, repetition of data is not commonly adopted to provide acceptable BERs in low SNR scenarios. One of the reasons is that the options mentioned above result in more complexity at the transmitter and/or receiver. The most practical option available for changing data quality from problematic to acceptable is to use error-control coding [2].

In this paper we propose a computationally efficient OFDM technique we will refer to as coherent Extended Symbol OFDM (ES-OFDM). First, coherent ES-OFDM is presented in section 2. Coherent ES-OFDM is able to achieve acceptable BERs at SNRs far below the noise floor. The question that rises then is how to synchronize to signals deeply buried in noise. In section 3, a synchronization algorithm is presented which can accurately estimate the time difference between transmitter and receiver at low SNR levels. In section 4, the performance of this algorithm is analyzed in case of an Additive White Gaussion Noise (AWGN) channel.

2 Coherent ES-OFDM

2.1 Model of coherent Modulation

Coherent ES-OFDM is based on the assumption that the receiver is exactly synchronized in time, frequency and phase. In Figure 1, the relevant parts of a base-band equivalent model of a coherent ES-OFDM based transmitter-receiver pair are presented.

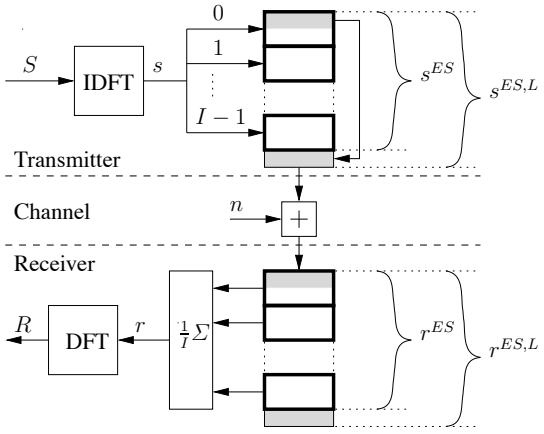

Fig. 1. Base-band equivalent model of coherent ES-OFDM

At the transmitter, a modulator produces S which consists of N complex values (indicated as S_f, $f = 0, 1, ..., N-1$), where each value is a constellation point from

a chosen modulation scheme. In this paper we restrict ourselves to BPSK. S is transformed into the time domain through the IDFT giving s.

$$s_t = \frac{1}{\sqrt{N}} \sum_{f=0}^{N-1} S_f e^{j\frac{2\pi ft}{N}}, \quad t = 0, 1, ..., N-1 \tag{1}$$

I copies of s are concatenated giving s^{ES}.

$$s_t^{ES} = s_{\mathrm{MOD}(t,N)}, \quad t = 0, 1, ..., IN-1 \tag{2}$$

where $\mathrm{MOD}(,\mathrm{N})$ indicates the modulo N operator. The last L samples of s ($L \leq N$) act as a cyclic prefix completing $s^{ES,L}$. The values of this extended symbol are shifted out serially and transmitted through the channel. Note that the word 'symbol' is used for representations in both the time and frequency domain. We assume an additive white Gaussian noise (AWGN) channel adding n to $s^{ES,L}$. In the receiver, the first step is to remove the cyclic prefix. The resulting extended symbol is r^{ES}.

$$r_t^{ES} = s_t^{ES} + n_t, \quad t = 0, 1, ..., IN-1 \tag{3}$$

The symbol r^{ES} consists of I blocks of N samples where each block consists of a replica of s and noise. The next step is to average these I blocks.

$$\begin{aligned} r_t &= \frac{1}{I} \sum_{i=0}^{I-1} r_{t+iN}^{ES}, \quad t = 0, 1, ..., N-1 \\ &= s_t + \frac{1}{I} \sum_{i=0}^{I-1} n_{t+iN} \end{aligned} \tag{4}$$

After averaging, the signal is transferred to the frequency domain by the DFT.

$$R_f = S_f + \frac{1}{I} \sum_{i=0}^{I-1} N_{f,i} \tag{5}$$

where

$$N_{f,i} = \mathrm{DFT}(n_{t+iN}), \quad i = 0, 1, ..., I-1 \tag{6}$$

In the next section we will analyze the BER performance when extending symbols.

Extending a symbol with a factor I implies that, at both the receiver and transmitter, the rate at which (I)DFTs are executed is reduced with the same factor I. At the receiver this reduction is slightly counteracted with a summation operation before the DFT. Note that extended symbols can also be generated by increasing the IDFT size with a factor I and only loading each Ith carrier with information. However, this is computationally inefficient compared to extending symbols as described above.

2.2 Bit Error Rates for coherent ES-OFDM

Extending the symbol at the transmitter and averaging at the receiver effectively does not affect the signal part s but averages the noise (expression 5). In an AWGN channel, the effect of averaging is that the noise power contribution is reduced with a factor I, see [6]. Hence, the SNR is increased with a factor I. Each doubling of the symbol extension factor I improves the SNR performance by approximately 3 dB which makes coherent ES-OFDM being able to operate at low SNR. Using the expression for the BER in case of BPSK in an AWGN channel (see [2]) results in

$$\mathrm{BER} = \frac{1}{2}\mathrm{erfc}(\sqrt{\frac{I}{M}\mathrm{SNR}}) \tag{7}$$

where $M = 1$ for BPSK.

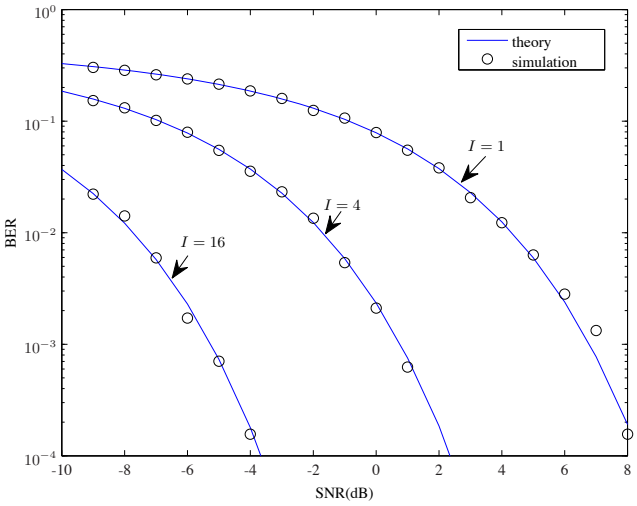

Fig. 2. BERs for coherent ES-OFDM for an AWGN channel.

In Figure 2, the theoretical and simulation results are presented for extension factors $I = 1, 4$ and 16. The simulation results are in correspondence with theory that each doubling of the factor I improves the BER performance with 3 dB (quadrupling leads to 6 dB improvement). We also see that synchronization has to be obtained at low SNR levels. For example to achieve 10^{-3} BER for $I = 16$, synchronization should be possible at an SNR of approximately -6 dB. Synchronization methods that use the correlation between the cyclic prefix and the 'tail' of the symbol (see [7], [8]) do not deliver the accuracy required; for negative SNR, the error is larger than one sample period. For that reason, we introduce a synchronization algorithm that can cope with negative SNR.

3 Synchronization

The synchronization of coherent ES-OFDM is based on the transmission of pilot symbols, known to both the transmitter and receiver. A prerequisite of the pilot symbol is that its autocorrelation function is the delta function in case of a critically sampled OFDM system. At the transmitter, the pilot symbol is defined as p_t for $t = 0, 1, ..., IN+L$. At the receiver, the pilot symbol is defined as $p_{\mathrm{MOD}(t,IN+L)}$ for $t \in \mathbb{Z}$. We assume that phase and frequency synchronization have been obtained and only time differences remain which are an integral number of sample intervals. The timing difference between transmitter and receiver then equals θ which is an integer number. The received signal is then defined as

$$r_{t,\theta}^{ES,L} = p_{(t+\theta)} + n_t, \quad t = 0, 1, ..., IN + L \tag{8}$$

In case of a critically sampled OFDM receiver and an AWGN channel, p_t and n_t can be considered as realizations of independent stochastic variables P and N, where samples are mutually independent (stochastic variables are indicated with non-italic capitals, realizations with corresponding lower case characters). Consequently, $r_{t,\theta}^{ES,L}$ is a realization of stochastic variable R = P+N. We define σ_{R}, σ_{P} and σ_{N} as the standard deviations of R, P and N respectively. The SNR of the received signal R then equals (see [9])

$$\mathrm{SNR} = \frac{\sigma_{\mathrm{P}}^2}{\sigma_{\mathrm{N}}^2} \tag{9}$$

Since P is an OFDM symbol, we approximate its probability density function by a normal distribution and therefore P and R have a bi-variate normal distribution. The correlation coefficient of this distribution equals

$$\rho = \sqrt{\frac{\mathrm{SNR}}{\mathrm{SNR}+1}} \tag{10}$$

The correlation function $z_{\tau,\theta}$ of $r_{t,\theta}^{ES,L}$ and p_t is defined as

$$z_{\tau,\theta} = \frac{1}{\sigma_{\mathrm{P}}\sigma_{\mathrm{R}} \cdot (IN+L)} \sum_{t=0}^{IN+L-1} r_{t+\theta}^{ES,L} \cdot p_{t+\tau}^{*} \tag{11}$$

where * indicates the complex conjugate. $z_{\tau,\theta}$ is a set of realizations of stochastic variables $\mathrm{Z}_{\tau,\theta}$ for $\tau = 0, 1, ..., IN + L - 1$.

Basically we are interested in the magnitudes of the complex values $z_{\tau,\theta}$. Note that the factor in front of the summation in expression 11 need not be calculated since we are only interested in the maximum of $|z_{\tau,\theta}|$. The maximum value of $|z_{\tau,\theta}|$ is obtained for $\tau = \theta$. Thus, the position of the maximum value of the magnitudes of the correlation function indicates the time difference between transmitter and receiver. We therefore formulate the following estimator

$$\tilde{\theta} = \arg\max_{\tau}\{|z_{\tau,\theta}|\} \tag{12}$$

4 Performance analysis

To asses the performance of the algorithm, we define $\sigma_{|\mathrm{Z}_{\tau,\theta}|}$ as the standard deviation and $\mu_{|\mathrm{Z}_{\tau,\theta}|}$ as the expected value of the magnitude of $\mathrm{Z}_{\tau,\theta}$. We observe that $\mu_{|\mathrm{Z}_{\tau,\theta}|} = \mu_{|\mathrm{Z}_{\tau-\theta,0}|}$ and $\sigma_{|\mathrm{Z}_{\tau,\theta}|} = \sigma_{|\mathrm{Z}_{\tau-\theta,0}|}$. So an analysis of the situation where $\theta = 0$ suffices to indicate the performance for any time difference. For that reason, we will omit the subscript θ in the remainder of this section. The expected value of $|\mathrm{Z}_\tau|$, $\mu_{|\mathrm{Z}_\tau|}$ will thus have a maximum at $\tau = 0$. Because of the critically sampled OFDM system and the AWGN channel, $\mu_{|\mathrm{Z}_\tau|}$ will mostly be zero except for a few values of τ. In case $I = 2$, this is illustrated in Figure 3.

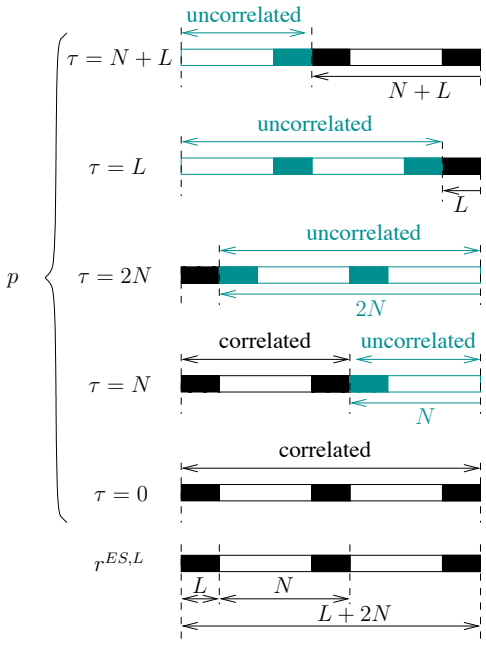

Fig. 3. Example of the construction of a correlation function

In this figure, the signal related part of the received signal $r^{ES,L}$ is shown at the bottom where the cyclic prefix of length L is presented at the left, followed by two symbols. Note that the tails of both symbols are equal to the cyclic prefix. Each sample of $r^{ES,L}$ is multiplied with a sample of p as described in expression 11. In Figure 3, $p_{t+\tau}$ is schematically drawn for those values of τ for which $\mu_{|z_\tau|} \neq 0$. In case $\tau = 0$, all samples of $r_\tau^{ES,L}$ are partly correlated with the corresponding samples of $p_{t+\tau}$. For $\tau = N$, the structure for $\tau = 0$ is cyclically shifted N positions to the left. Consequently, the first $L + N$ samples are still correlated with $r^{ES,L}$ (at the bottom of Figure 3) but the last N samples are uncorrelated. For $\tau = 2N$ the last $2N$ samples are

uncorrelated. In case $\tau = L$, the first $2N$ samples are uncorrelated leading to the same expected value of $|z_\tau|$ as for $\tau = 2N$. The correlation peak for $\tau = N + L$ equals the peak for $\tau = N$. In general, $\mu_{|\mathrm{Z}_\tau|}$ has a maximum value for $\tau = 0$ and has smaller peak values for $\tau = iN,\ \ i = 1, 2, ..., I$ and $\tau = jN + L,\ \ j = 0, 1, ..., N - 1$.

Because of the addition of noise and because the summation in expression 11 runs over a finite length, a realization of $|\mathrm{Z}_\tau|$ might have its maximum for other values than $\tau = 0$. This is indicated as an erroneous detection. To evaluate the performance of the synchronization algorithm, we determine the probability of erroneous detection ($\mathrm{P_E}$). For convenience, we first determine the probability that the peak is detected correctly ($\mathrm{P_D}$). The peak is detected correctly if $\forall\tau \neq 0,\ \ |z_\tau| < |z_0|$, thus

$$\mathrm{P_D} = \prod_{\tau=1}^{IN+L-1} \mathrm{P}(|z_\tau| < |z_0|) \tag{13}$$

To determine $\mathrm{P_D}$, we have to determine the probability distribution of $|\mathrm{Z}_\tau|$. We start with the definition of four partial sums x_τ, y_τ, $x\mathrm{o}_\tau$ and $y\mathrm{o}_\tau$. After that, the probability distribution will be determined.

As suggested in Figure 3, the summation in expression 11 is split into two parts; a summation of products of $r^{ES,L}$ and p where there is correlation and a summation of products where there is no correlation. For $\tau = 1, 2, ..., IN+L-1$, we therefore define x_τ, the first part of the summation, and y_τ, the second part of the summation.

$$\begin{aligned} x_\tau &= \frac{1}{\sigma_\mathrm{P}\sigma_\mathrm{R} \cdot (IN + L - \tau)} \sum_{t=0}^{IN+L-\tau-1} r_t^{ES,L} \cdot p_{t+\tau}^* \\ y_\tau &= \frac{1}{\sigma_\mathrm{P}\sigma_\mathrm{R} \cdot \tau} \sum_{t=IN+L-\tau}^{IN+L-1} r_t^{ES,L} \cdot p_{t+\tau}^* \end{aligned} \tag{14}$$

For $\tau = iN,\ \ i = 1, 2, ..., I$, x_τ is the correlated part and y_τ is the uncorrelated part. For $\tau = jN + L,\ \ j = 0, 1, ..., I - 1$, it is the other way around.

We also split the summation in expression 11 into two parts for the specific case where $r^{ES,L}$ and p are aligned in time

$$\begin{aligned} x\mathrm{o}_\tau &= \frac{1}{\sigma_\mathrm{P}\sigma_\mathrm{R} \cdot (IN + L - \tau)} \sum_{t=0}^{IN+L-\tau-1} r_t^{ES,L} \cdot p_t^* \\ y\mathrm{o}_\tau &= \frac{1}{\sigma_\mathrm{P}\sigma_\mathrm{R} \cdot \tau} \sum_{t=IN+L-\tau}^{IN+L-1} r_t^{ES,L} \cdot p_t^* \end{aligned} \tag{15}$$

In both $x\mathrm{o}_\tau$ and $y\mathrm{o}_\tau$, p and $r^{ES,L}$ are correlated.

To determine $\mathrm{P_D}$ (expression 13), the probalility distribution of $|\mathrm{Z}_\tau|$ has to be determined for each τ. We distinguish 3 disjunct sets of values for τ. For τ-set 1, $\tau = iN$, $i = 1, 2, ..., I$. For τ-set 2, $\tau = jN + L$, $j = 0, 1, ..., I - 1$ and τ-set 3 consists of all other values of τ. We will analyse the probability distributions of $|\mathrm{Z}_\tau|$ for the three τ-sets separately, followed by an overall analysis.

4.1 Analysis of τ-set 1

For $\tau = iN,\ \ i = 1, 2, ..., I, x_{iN}$ equals xo_{iN} because the summations over the correlated parts lead to identical results. The difference between z_{iN} and z_0 is caused by the summation over the uncorrelated part; y_{iN} and yo_{iN}. Relying on the Central Limit Theorem, $|y_{iN}|$ and $|yo_{iN}|$ can be considered as realizations of normally distributed Gaussian processes (see [10]): $\mathrm{U}_{iN} \sim \mathcal{N}(\mu_{|Y_{iN}|}, \sigma^2_{|Y_{iN}|})$ and $\mathrm{C}_{iN} \sim \mathcal{N}(\mu_{|Yo_{iN}|}, \sigma^2_{|Yo_{iN}|})$ respectively. A detection is correct if $|y_{iN}| < |yo_{iN}|$. The probability of correct detection is then $\mathrm{P}(\mathrm{U}_{iN} < \mathrm{C}_{iN})$ or $\mathrm{P}(\mathrm{T}_{iN} < 0)$, $\mathrm{T}_{iN} = \mathrm{U}_{iN} - \mathrm{C}_{iN}$. T_{iN} has a $\mathcal{N}(\mu_{\mathrm{T}_{iN}}, \sigma^2_{\mathrm{T}_{iN}})$ distribution, where

$$\mu_{\mathrm{T}_{iN}} = \mu_{|Y_{iN}|} - \mu_{|Yo_{iN}|} = 0 - \rho = -\rho \tag{16}$$

$$\begin{aligned} \sigma^2_{\mathrm{T}_{iN}} &= \sigma^2_{|Y_{iN}|} + \sigma^2_{|Yo_{iN}|} \\ &= \frac{1}{2iN} + \frac{1+\rho^2}{2iN} = \frac{\rho^2+2}{2iN} \end{aligned} \tag{17}$$

The probability of correct detection for $\tau = iN,\ \ i = 1, 2, ..., I$, then becomes

$$\mathrm{P}(|z_\tau| < |z_0|) = \mathrm{P}(\mathrm{T}_{iN} < 0) = \frac{1}{2}\left(1 + \mathrm{erf}\left(\frac{-\mu_{\mathrm{T}_{iN}}}{\sigma_{\mathrm{T}_{iN}}\sqrt{2}}\right)\right) \tag{18}$$

where erf is the error function.

4.2 Analysis of τ-set 2

For $\tau = jN + L,\ \ j = 0, 1, ..., I-1, \mathrm{P}(|z_{jN+L}| < |z_0|) = \mathrm{P}(|z_{(I-j)N}| < |z_0|)$. So, the contributions to expression 13 for $\tau = jN + L,\ \ j = 0, 1, I-1$ are equal to the contributions for $\tau = iN,\ \ i = 1, 2, ..., I$.

4.3 Analysis of τ-set 3

For all other values of τ, the probability distributions of $|\mathrm{Z}_\tau|$ are equal to a Rayleigh distribution and an estimate of the probability of detection is based on [10]

$$\mathrm{P}(|z_\tau| < |z_0|) = 1 - e^{-\rho^2(IN+L)} \tag{19}$$

4.4 Overall analysis

The overall probability of detection as given in expression 13, is then approximated by

$$\begin{aligned} \mathrm{P_D} = \left(\prod_{i=1}^{I}\left(\frac{1}{2}\left(1 + \mathrm{erf}\left(\frac{-\mu_{\mathrm{T}_{iN}}}{\sigma_{\mathrm{T}_{iN}}\sqrt{2}}\right)\right)\right)^2\right) \\ \cdot\left(1 - e^{-\rho^2(IN+L)}\right)^{(N-2)I} \end{aligned} \tag{20}$$

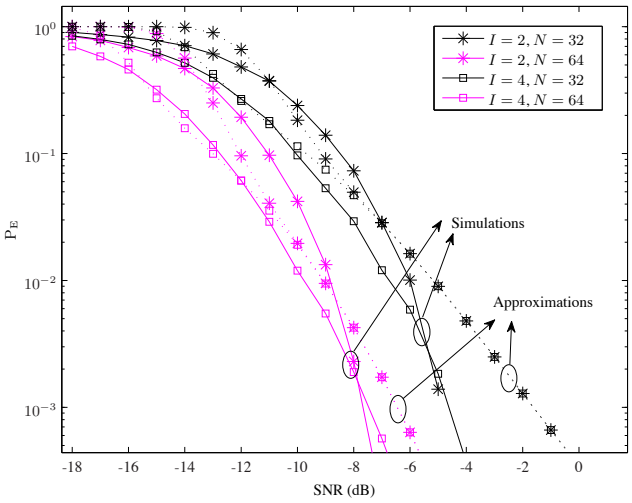

Fig. 4. BERs for coherent ES-OFDM for an AWGN channel.

The probability of error (P_E = 1-P_D) is given in Figure 4 for $I = 2$ and $I = 4$. For both cases, P_E is given for $N = 32$ and $N = 64$. The approximations are given by dashed lines, whereas simulation results are given by solid lines.

As can be seen from Figure 4, the simulation results match reasonably well with the approximations. We explain the differences between simulations and approximations by realizing that we assume that extended OFDM symbols and the values of the correlation function z_τ have a Gaussian probability distribution but in practice they have not. Especially for a small number of carriers, this assumption is violated. This is confirmed by the observation that the approximations for $N = 64$ give a better match with the simulations than the approximations for $N = 32$. Furthermore, if we concentrate on situations where $P_E < 10^{-3}$, increasing the number of carriers has more effect than increasing the symbol extension factor I. For these low P_E values, the second part within expression 20 has limited influence. We therefore concentrate on the first part. The influence of I and N is effectuated through $\sigma_{T_{iN}}$. Increasing N will increase each element of the product in expression 20 whereas increasing I will only add one element to the product, resulting in smaller increase of P_D.

We conclude that the proposed synchronization algorithm can cope with low SNR scenarios. However, for a fixed number of carriers, the symbol extension factor I cannot be increased infinitely since synchronization performance does not scale with I.

5 Conclusion

By extending symbols, OFDM can be used to achieve acceptable BERs at low SNR. In case of coherent ES-OFDM, the SNR can be lowered by 3 dB each time the symbol

length is doubled (and inherently, the data rate is halved). Acceptable BERs can be achieved far below the noise floor.

In this paper, an algorithm is presented which estimates the time difference between transmitter and receiver under the assumption that phase and frequency synchronization have been obtained. It makes use of (extended) pilot symbols and can achieve accurate estimates at negative SNRs. Both theoretical approximations as well as simulation results are presented. For example, for an extension factor 4 ($I = 4$), the probability that the time difference is not correctly estimated is less than 10^{-3} in case of 64 carriers and SNR = -6 dB.

The algorithm has been analyzed for an AWGN channel. Future work will be to use more realistic channel models. Furthermore, implementation aspects of the algorithm will have to be investigated.

References

1. A. Bahai, B. Saltzber, and M. Ergen, *Multi-carrier Digital Communication: Theory and Applications*, 2nd ed. Springer, 2004.
2. S. Haykin, *Communication Systems*, 4th ed. John Wiley & Sons, Inc., 2001.
3. N. Maeda, H. Atarashi, S. Abeta, and M. Sawahashi, "Throughput comparison between vsf-ofcdm and ofdm considering effect of sectorization in forward link broadband packet wireless access," *Vehicular Technology Conference, 2002. Proceedings. VTC 2002-Fall. 2002 IEEE 56th*, vol. 1, pp. 47–51 vol.1, 2002.
4. B. Gaffney, A. Fagan, and S. Rickard, "Upper bound on the probability of error for repetition mb-ofdm in the rayleigh fading channel," *Ultra-Wideband, 2005. ICU 2005. 2005 IEEE International Conference on*, pp. 4 pp.–, Sept. 2005.
5. L. Medina and H. Kobayashi, "Proposal of ofdm system with data repetition," *Vehicular Technology Conference, 2000. IEEE VTS-Fall VTC 2000. 52nd*, vol. 1, pp. 352–357 vol.1, 2000.
6. W. L. Davenport, W. B. Root, *An Introduction to the Theory of Randam Signals and Noise*. John Wiley & Sons, 1987.
7. J. van de Beek, M. Sandell, and P. Borjesson, "Ml estimation of time and frequency offset in ofdm systems," *Signal Processing, IEEE Transactions on*, vol. 45, no. 7, pp. 1800 –1805, jul 1997.
8. J.-J. van de Beek, P. Borjesson, M.-L. Boucheret, D. Landstrom, J. Arenas, P. Odling, C. Ostberg, M. Wahlqvist, and S. Wilson, "A time and frequency synchronization scheme for multiuser ofdm," *Selected Areas in Communications, IEEE Journal on*, vol. 17, no. 11, pp. 1900–1914, Nov 1999.
9. J. Stuart, A. & Ord, *Kendall's advanced theory of statistics*, 5th ed. Charles Griffin & company, 1987, vol. 1.
10. K. Milne, "Theoretical performance of a complex cross-correlator with gaussian signals," *Radar and Signal Processing, IEE Proceedings F*, vol. 140, no. 1, pp. 81 –88, feb 1993.